Hypertonic Media Inhibit Receptor-mediated Endocytosis by Blocking Clathrin-coated Pit Formation

John E. Heuser* and Richard G. W. Anderson‡

*Department of Cell Biology and Physiology, Washington University School of Medicine, St. Louis, Missouri 63110; and
‡Department of Cell Biology, The University of Texas Southwestern Medical Center, Dallas, Texas 75235

Abstract. Two seemingly unrelated experimental treatments inhibit receptor mediated endocytosis: (*a*) depletion of intracellular K^+ (Larkin, J. M., M. S. Brown, J. L. Goldstein, and R. G. W. Anderson. 1983. *Cell.* 33:273–285); and (*b*) treatment with hypertonic media (Daukas, G., and S. H. Zigmond. 1985. *J. Cell Biol.* 101:1673–1679). Since the former inhibits the formation of clathrin-coated pits (Larkin, J. M., W. D. Donzell, and R. G. W. Anderson. 1986. *J. Cell Biol.* 103:2619–2627), we were interested in determining whether hypertonic treatment has the same effect, and if so, why. Fibroblasts (human or chicken) were incubated in normal saline made hypertonic with 0.45 M sucrose, then broken open by sonication and freeze-etched to generate replicas of their inner membrane surfaces. Whereas untreated cells display typical geodesic lattices of clathrin under each coated pit, hypertonic cells display in addition a number of empty clathrin "microcages". At first, these appear around the edges of normal coated pit lattices. With further time in hypertonic medium, however, normal lattices largely disappear and are replaced by accumulations of microcages. Concomitantly, low density lipoprotein (LDL) receptors lose their normal clustered distribution and become dispersed all over the cell surface, as seen by fluorescence microscopy and freeze-etch electron microscopy of LDL attached to the cell surface. Upon return to normal medium at 37°C, these changes promptly reverse. Within 2 min, small clusters of LDL reappear on the surfaces of cells and normal clathrin lattices begin to reappear inside; the size and number of these receptor/clathrin complexes returns to normal over the next 10 min. Thus, in spite of their seeming unrelatedness, both K^+ depletion and hypertonic treatment cause coated pits to disappear, and both induce abnormal clathrin polymerization into empty microcages. This suggests that in both cases, an abnormal formation of microcages inhibits endocytosis by rendering clathrin unavailable for assembly into normal coated pits.

CLATHRIN coated pits are the primary plasma membrane specialization involved in the uptake of a wide variety of molecules by receptor-mediated endocytosis (4, 38). Two broad functions have been attributed to these regions of membrane: (*a*) molecular determinants associated with the clathrin lattice may cause receptors to become clustered; and (*b*) the clathrin lattice may in some way control the invagination of the membrane to form endocytic vesicles. To understand the molecular mechanisms underlying these two aspects of coated pit function, one approach is to search for treatments that inhibit endocytosis and then to characterize the effects of these treatments on coated pit structure and receptor clustering.

Currently, three experimental treatments are known to inhibit receptor-mediated endocytosis: (*a*) depletion of intracellular potassium (22, 24–26, 29, 30, 34, 40), (*b*) exposure of cells to hypertonic media (10), and (*c*) acidification of the cytoplasm (11, 16, 21, 41). Whereas potassium depletion appears to inhibit the assembly of coated pits, causing the cell to have a plasma membrane virtually devoid of endocytic sites (24, 26, 34), acidification appears not to affect assembly but to arrest the pinching off of coated pits to form coated vesicles (11, 41). Whether or not hypertonic treatment exerts its effects by interfering with one or another of these aspects of coated pit function has not been determined.

Daukas and Zigmond (10) first showed that exposure of polymorphonuclear leukocytes to media containing 0.43 M sucrose caused the rapid and reversible inhibition of receptor-mediated internalization of chemotactic peptides, suggesting that coated pit function was inhibited by hypertonicity. We further analyze the effects of hypertonic media on coated pit function and architecture in cultured fibroblasts, taking advantage of the opportunity to obtain distinct en face images of coated pits via the quick-freeze/deep-etch method of preparing cells for electron microscopy (15, 17). This shows that hypertonic treatment rapidly and reversibly inhibits the internalization of low density lipoprotein (LDL)[1] and causes the receptors for this ligand to become randomly

1. *Abbreviations used in this paper*: HRP, horseradish peroxidase; LDL, low density lipoprotein.

dispersed on the plasma membrane. Coordinately, coated pits become reduced in size and number, and many small "microcages" of clathrin appear on the inner membrane surface. These unusual polymers, sharply curved and devoid of membrane, become so abundant that they apparently deplete the cytoplasm of clathrin needed for normal coated pit assembly. In this sense, hypertonicity and potassium depletion appear to inhibit endocytosis in the same way. It remains to be seen, however, whether both treatments stimulate clathrin microcage formation by the same mechanism.

Materials and Methods

Materials

DME (No. 320-185) and MEM (No. 180-173) were purchased from Gibco Laboratories (Grand Island, NY). A mixture of insulin, transferrin, and selenium (ITS Premix) was purchased from Collaborative Research, Inc. (Lexington, MA). Human LDL (d = 1.019–1.063 g/ml) and lipoprotein-deficient serum (d > 1.215 g/ml) were prepared by ultracentrifugation of plasma (12). Fluorescent LDL (designated r[PMCA Oleate] LDL) was prepared as previously described (6). Poly-L-lysine (cat. No. P-2636) and horseradish peroxidase Type VI (cat. No. H-1784) were from Sigma Chemical Co. (St. Louis, MO). Anti-mouse IgG conjugated to fluorescein isothiocyanate was from Zymed (cat. No. 61-6511). All fixatives were from Ladd, Inc. (Burlington, VT). Monoclonal anti-clathrin heavy chain ("×22") was a generous gift from Francis Brodsky (7). Other supplies were obtained from sources as previously reported (24).

Cell Culture

Cultured human fibroblasts were derived from a skin biopsy obtained from a normal subject. Cells were grown in monolayer and set up for experiments according to a standard format (12). On day zero, 3–4 × 10^4 cells were seeded in each petri dish (60 × 15 mm) that contained a 22-mm^2 coverslip, then cultured in 3 ml of DME supplemented with 100 U/ml penicillin, 100 mg/ml of streptomycin, and 10% (vol/vol) FCS. Fresh medium of the same composition was added on day three. On day five of cell growth, each monolayer received 2 ml DME supplemented with penicillin, streptomycin, 5 μg/ml insulin, 5 μg/ml transferrin, 5 mg/ml selenium, and 10% (vol/vol) human lipoprotein-deficient serum. All experiments were performed on day seven after 48 h of incubation in this lipoprotein-deficient serum.

Cultured chicken fibroblasts were removed from primary culture with trypsin/EDTA and replated at 10^5 cells/ml into 35-mm petri dishes containing several 3 × 3-mm pieces of No. 1 glass coverslips that were cleaned in hot chromic acid, washed extensively with water, and sterilized with ethanol before use. The cells were maintained in MEM supplemented with 10% FCS, 100 U/ml of penicillin, and 100 mg/ml of streptomycin. After one day of culture at 37°C, at a time when the cells had spread and reached subconfluence on the small glass squares, they were removed from the CO_2 incubator and washed four times at 37°C in Ringer's solution (prepared according to a standard formula [19]) before further experimental manipulation.

Preparation of Carbon–Platinum Replicas of the Inner Cell Surface

Cells on coverslips were subjected to various experimental treatments detailed in Results and the figure legends. At the end of each treatment, each coverslip was exposed for 5 s to 0.3 mg/ml poly-L-lysine (molecular mass ~47 kD; Sigma Chemical Co.) dissolved in the experimental solution. The cells were then washed 10 s in hypotonic medium, prepared by mixing one part experimental solution with two parts distilled water. The cells were then transferred to buffer A (70 mM KCl, 30 mM Hepes, pH 7.2, 5 mM $MgCl_2$, 3 mM EGTA) and immediately broken open by placing an ultrasonic microprobe (Kontes Co., Vineland, NJ) 4 mm away from the surface of the coverslip and delivering 15% maximum power for 1 s. Sonicated cells were immediately transferred to 2% glutaraldehyde in buffer A for 30 min at room temperature. After fixation, the coverslips were washed four times with distilled water in preparation for freeze-drying (18). Thereafter, each coverslip was placed on a slab of aldehyde-fixed rabbit lung and attached to the plunger of the "Cryopress" freezing machine (Med-Vac, Inc., St. Louis, MO). Excess water was blotted from the coverslip just before it was brought into contact with a copper block cooled with liquid helium, as previously described (13, 20). The frozen coverslip was then transferred to a freeze-etch unit (No. 301 or 400; Balzers S. P. A., Milan) and freeze-dried at −80°C for 15 min. A rotary replica of its exposed surface was prepared by evaporating 2–3 nm of platinum–carbon onto it at an angle of 24° above the horizontal, followed by 10 nm of pure carbon rotary evaporated at a 75° angle. The replica was then separated from the coverslip by immersion in full strength hydrofluoric acid, washed twice in distilled water, and cleaned by flotation on household bleach (5% sodium hypochlorite) for 5–10 min. Finally, it was washed several times in distilled water, broken into small pieces, and picked up on 400-mesh Formvar-coated grids for electron microscopy.

Fluorescence Microscopy

To monitor receptor-mediated endocytosis of LDL, fibroblast monolayers grown on glass coverslips for 7 d were subjected to the experimental protocols indicated in the appropriate figure legends. At the end of each experiment, 20 μg/ml of r(PCMA oleate) LDL was added to each dish and cells were incubated at 37°C for 30 min. Then the cells were fixed for 20 min at room temperature in 3% (wt/vol) paraformaldehyde in buffer B (10 mM Na phosphate, 150 mM NaCl, and 2 mM $MgCl_2$ at pH 7.4).

To localize clathrin distribution by indirect immunofluorescence, fibroblast monolayers grown on glass coverslips were subjected to experimental treatments described in the figure legends and then fixed with 2% (wt/vol) paraformaldehyde in buffer B. The cells were then washed briefly with 2 ml of 50 mM NH_4Cl in buffer B and twice more with buffer B. Each monolayer was then permeabilized with 2 ml of 0.01% (vol/vol) Triton X-100 in buffer B for 5 min at 10°C. Each coverslip was then placed in a petri dish (cell side up), covered with 60 μl of mouse anti-clathrin IgG (1 μg/ml of monoclonal anti-heavy chain antibody [×22; reference 7]) and incubated for 60 min at 37°C. After four washes (15 min each) with buffer B, the cells were incubated with 60 μl of goat anti-mouse IgG conjugated to fluorescein isothiocyanate (50 μg/ml) for 60 min at 37°C. The coverslips were finally washed and mounted on glass slides with DABCO media or with 0.1 M *N*-propyl gallate (Sigma Chemical Co.) in 70% glycerol/30% buffer B. All fluorescence samples were viewed with UV epi-illumination using the appropriate filter packages (5, 6).

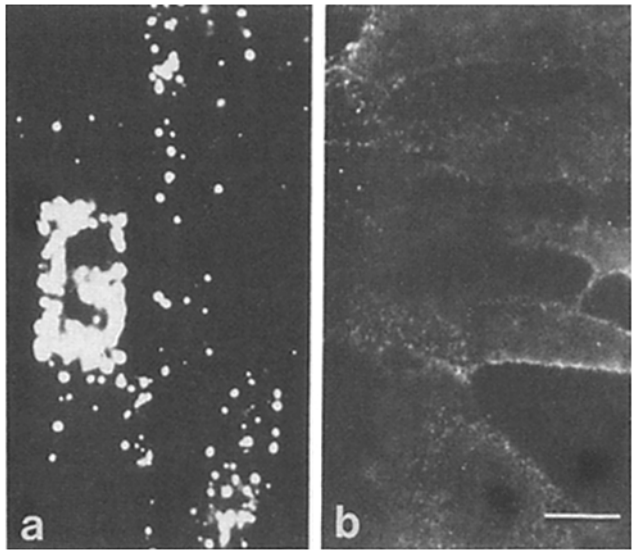

Figure 1. (*a*) Control distribution of fluorescent LDL in human fibroblasts. Cells were grown in media that induce LDL receptors, then incubated in 50 μg/ml r(PMCA Oleate) LDL for 30 min at 37°C; this demonstrates normal LDL uptake into large endosomes via receptor-mediated endocytosis. (*b*) Fluorescent LDL in hypertonically treated fibroblasts. Cells were pretreated with HBSS containing 0.45 M sucrose for 15 min at 37°C. To this hypertonic medium, r(PMCA Oleate) LDL was added at 50 μg/ml and the cells were incubated for a further 30 min at 37°C before fixation. This demonstrates that hypertonicity stops LDL endocytosis and yields a diffuse distribution of LDL on the cell surface. Bar, 10 μm.

Internalization of Horseradish Peroxidase

Horseradish peroxidase (HRP) uptake was analyzed as previously described (19). Cultured chick fibroblasts grown on full-sized, 22-mm^2 coverslips were subjected to the indicated treatment and then fixed with 2% formaldehyde and 0.25% glutaraldehyde in Ringer's solution for 1 h. The cells were then processed for visualization of peroxidase with diaminobenzidine and H_2O_2 as previously described (19).

Surface Distribution of LDL Binding Sites

To monitor the distribution of LDL receptors, replicas were prepared of freeze-dried human fibroblasts that had been incubated for various times with native LDL. Human fibroblasts grown in culture for 7 d as above were either chilled to 4°C in Hank's balanced salt solution (HBSS) or preincubated for 45 min at 37°C in HBSS containing 0.43 M sucrose before chilling to 4°C. Both sets of cells were then incubated at 4°C for 1 h in HBSS containing 20 μg/ml of LDL. Cells were then washed with HBSS containing 1% BSA according to standard procedures (12) and either fixed immediately or warmed up to 37°C for the indicated periods of time before fixation. In all cases, cells were fixed with 2% glutaraldehyde in HBSS for 30 min at room temperature, washed in HBSS, and shipped to St. Louis by Federal Express. The next day, samples were subjected to quick-freezing, freeze-drying, and rotary replication with platinum at 24°C as described above.

Electron Microscopy

All electron micrographs were prepared using a JEOL 200CX electron microscope operating at 100 KV. Stereo viewing and digitization and quantification of the micrographs were carried out as previously described (13, 17).

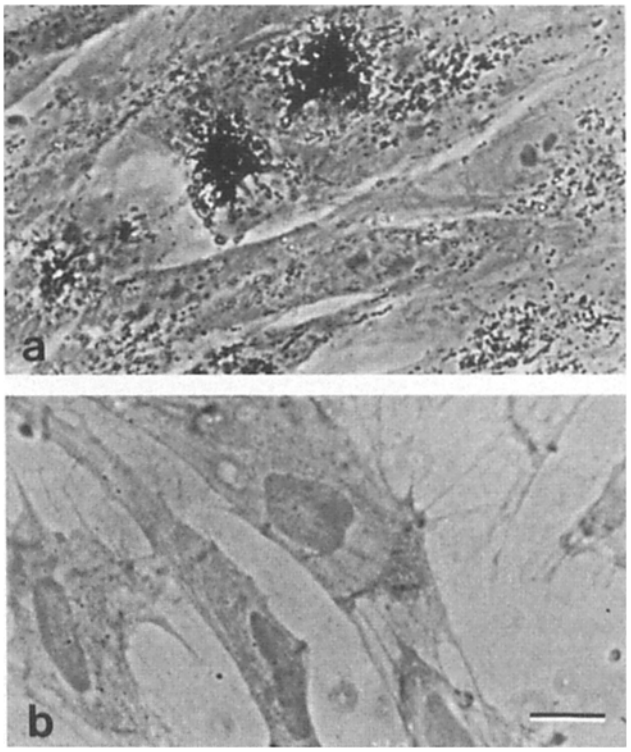

Figure 2. HRP uptake by chick fibroblasts in culture. All cells were exposed to 10 mg/ml HRP for 30 min at 37°C, then washed free of extracellular HRP, fixed, and incubated with diaminobenzidine/H_2O_2 to demonstrate intracellular sites of HRP accumulation (dark granules). *a* illustrates control cells in normal, isosmotic media. *b* illustrates cells pretreated with 0.45 M sucrose for 5 min before and 30 min during HRP exposure. In contrast to the normal uptake of HRP seen in *a*, hypertonically treated cells are essentially devoid of HRP. Bar, 10 μm.

Results

Hypertonic Media Inhibit Receptor-mediated Endocytosis of LDL and Bulk Uptake of HRP

To determine if hypertonic media would inhibit endocytosis of LDL, endocytosis was monitored using fluorescent LDL (6). Normal human fibroblasts exposed to fluorescent LDL for 30 min at 37°C internalized the ligand into numerous vacuoles located in the perinuclear area (Fig. 1 *a*). In contrast, cells pretreated with hypertonic medium for 15 min at 37°C and then incubated with fluorescent LDL in the same medium for 30 min at 37°C, displayed few or no fluorescent vacuoles inside (Fig. 1 *b*); instead, fluorescence appeared to be diffusely distributed on their surfaces. Likewise, HRP uptake into chick fibroblasts was inhibited by hypertonicity. After 20 min of incubation in 10 mg/ml HRP, the tracer was found in numerous vesicles within the cytoplasm of untreated cells (Fig. 2 *a*). In contrast, HRP accumulation was virtually absent in cells pretreated with hypertonic media for 10 min and then maintained in hypertonic media during a 30-min exposure to the tracer (Fig. 2 *b*). These data indicate that in fibroblasts, hypertonicity inhibits both receptor-mediated and bulk-phase endocytosis (cf. reference 29). This is in contrast to leukocytes, where bulk phase uptake is apparently relatively unaffected (10).

Effects of Hypertonic Treatment on Coated Pits

Human and chick fibroblasts processed for indirect immunofluorescence localization of clathrin normally displayed a characteristic punctate distribution of staining on their top and bottom membrane surfaces, as well as internal perinu-

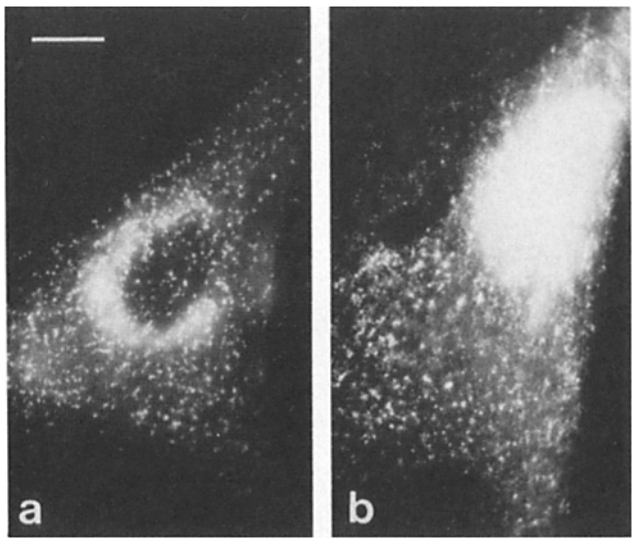

Figure 3. Indirect immunofluorescent localization of clathrin in human fibroblasts. Cells were formaldehyde fixed, permeabilized, and processed for localization of clathrin heavy chain with a monoclonal IgG (7). In control cells (*a*), anti-clathrin staining occurs at discrete spots on the top and bottom surface and as an internal perinuclear halo that presumably represents the Golgi apparatus. In cells treated with 0.45 M sucrose for 30 min at 37°C (*b*), subsurface staining of clathrin appears to be more irregular and less distinctly punctate than normal, while perinuclear staining is increased. Bar, 10 μm.

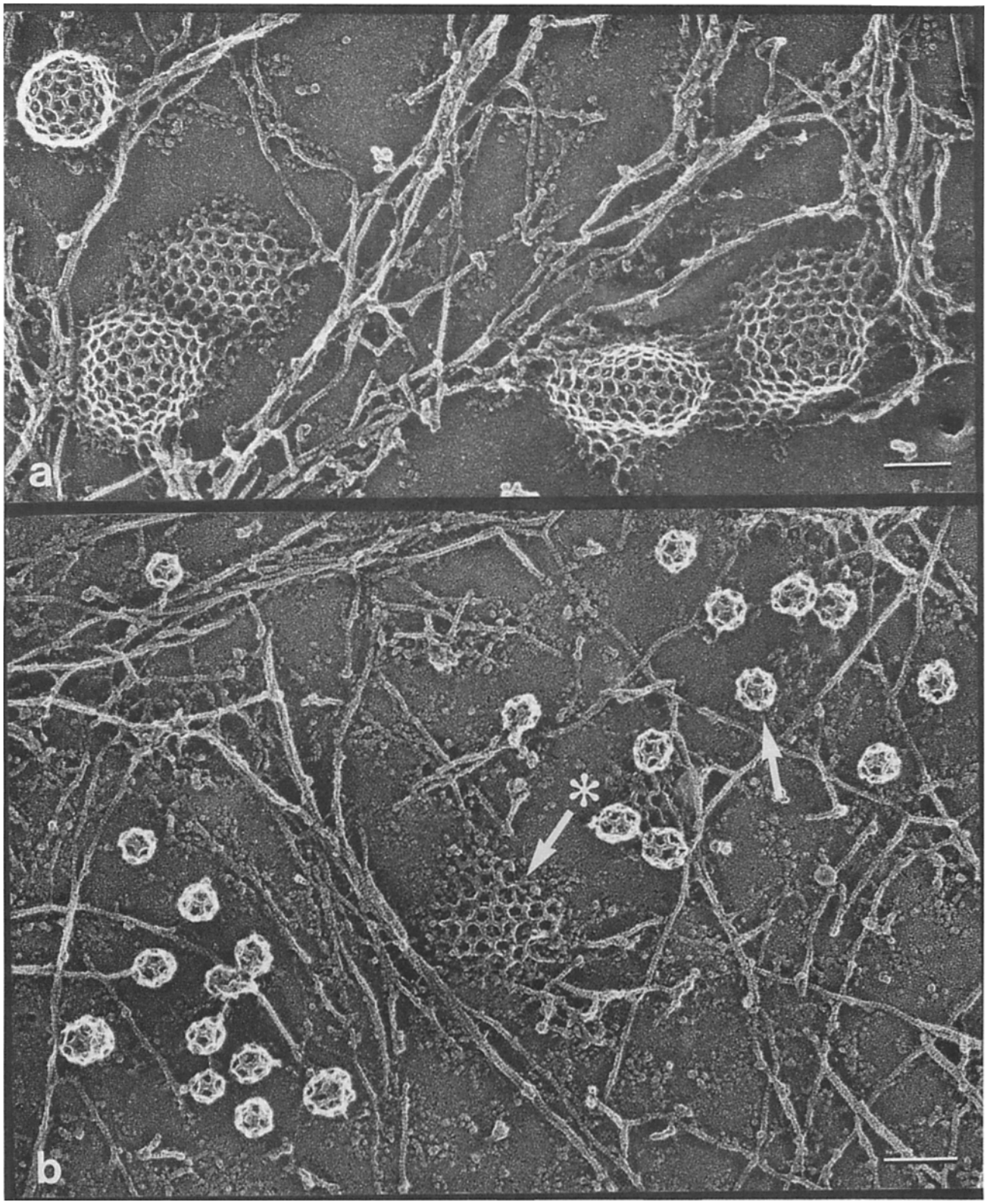

Figure 4. Survey views of clathrin lattices on the inner surface of a normal chick fibroblast (*a*), compared with lattices on a fibroblast exposed to 0.45 M sucrose for 30 min at 37°C (*b*). In normal cells, various stages of clathrin lattice assembly and curvature are seen. In hypertonic cells, membrane-attached lattices are reduced to flat remnants (such as the one at the asterisk) and are replaced by numerous clathrin microcages (one of which is indicated by the arrow). Bar, 0.1 μm.

Table I. Relative Curvature of Clathrin Lattices

Duration of	Total No. of lattices evaluated*	Small and flat	Normal-sized, flat	Gently curved	Hemi-spherical	Almost completely spherical
Hypertonic treatment (min)						
0′ (control)	98	0.05‡	0.15	0.25	0.20	0.30
10′	58	0.35	0.25	0.15	0.10	0.15
30′	61	0.70	0.10	0.10	0.05	0.00
Recovery (min)						
5′	54	0.55	0.15	0.05	0.15	0.15
15′	91	0.15	0.20	0.10	0.30	0.25

* Representing all of the lattices that were present on a total of ~50 μm^2 of membrane surface area, i.e., on 20 electron micrographs taken at 50,000×, of fields chosen for technical quality rather than for any specific feature of cell structure.
‡ These values represent fractions of the total number of lattices evaluated, rounded off to the nearest 0.05, so the total is not necessarily 1.00.

clear staining in the Golgi area (Fig. 3 *a*). In contrast, hypertonically treated cells displayed fewer and more irregular punctae of clathrin immunoreactivity at the cell surface (Fig. 3 *b*). To some extent, this reduction in staining may have been only apparent, since hypertonically treated cells also displayed increased diffuse fluorescence, particularly around their nuclei.

Higher resolution views of these changes in clathrin distribution were obtained from platinum replicas of the inner surfaces of freeze-dried chick fibroblast membranes. Untreated cells had numerous clathrin lattices distributed on the inner membrane surface (Fig. 4 *a*). Normally, these displayed a range of shapes, from almost flat to almost completely spherical (Table I). Normal lattice diameter was 0.15–0.2 μm, hence each lattice was composed of several dozen clathrin polygons (cf. references 15 and 17). In contrast, when cells were incubated in hypertonic media for 30 min, the number of coated pits as well as their size was dramatically reduced (Fig. 4 *b* and Table I). The remaining lattices averaged 0.08 μm in diameter, had a relatively planar configuration, and typically consisted of only 5–10 polygons.

Also evident on the membranes of hypertonically treated chick fibroblasts were many extremely small (50–70-nm-diam) and extremely round geodesic lattices (Fig. 4 *b*). These unusual polymers we presume to be clathrin and henceforth will term "microcages". They were most abundant at the margins of the remaining flat lattices (*arrows* in Fig. 5), but also occurred elsewhere on the membrane, though in no particular association with actin filaments or other plasma membrane features. These microcages looked exactly like the small lattices that form when purified clathrin triskelions are polymerized via exposure to low pH (9, 23). Also, they looked just like the smallest of the cages typically found in purified preparations of brain coated vesicles (8, 37). These

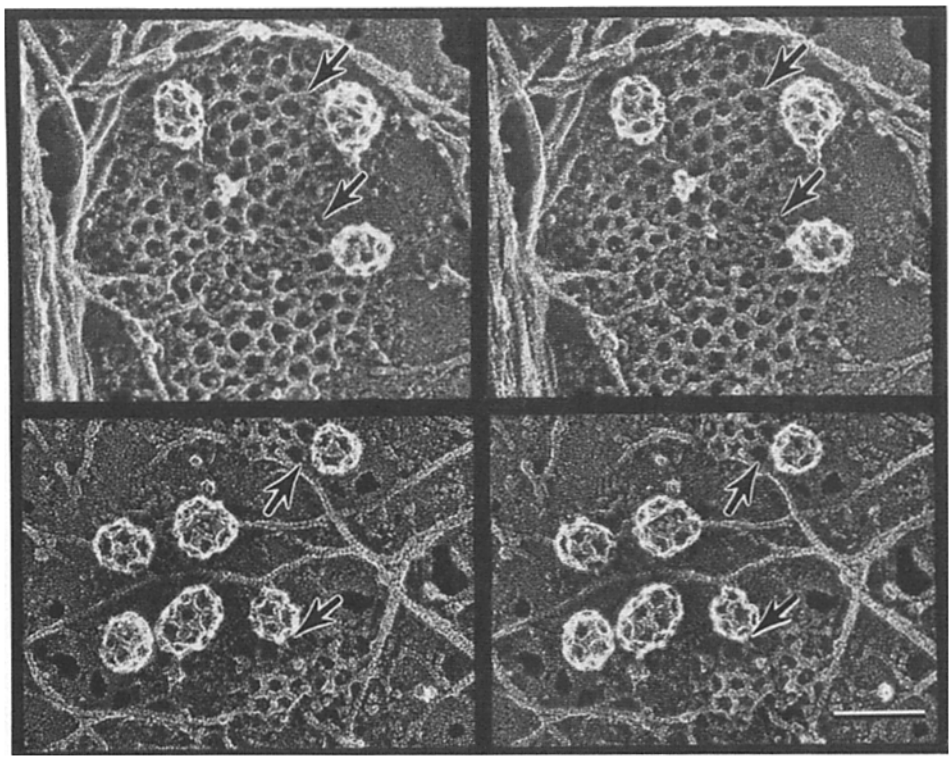

Figure 5. Two stereo views of microcages in association with residual clathrin lattices from chick fibroblasts treated with hypertonic sucrose for 30 min at 37°C. Note that microcages often but not invariably appear to connect to the margins of the residual lattices (*arrows*). See reference 16 for analysis of why this occurs. Bar, 0.1 μm.

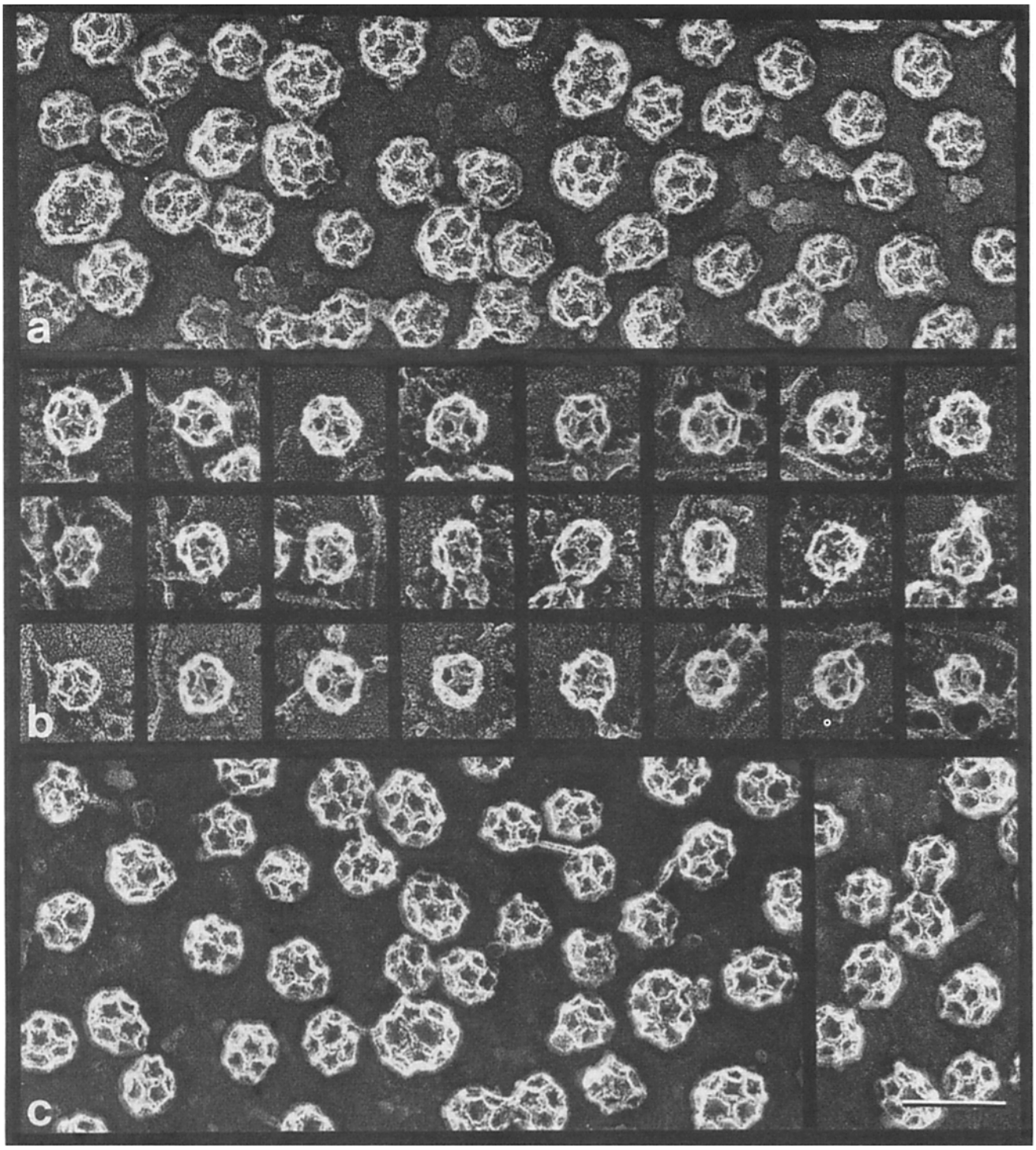

Figure 6. Comparison between the microcages formed in vivo during hypertonic treatment (*b*), cages generated by in vitro dialysis of clathrin plus assembly polypeptides into pH 6.5 buffer (*a*; cf. reference 48), and a typical brain coated vesicle preparation (*c*). All are printed at the same magnification to illustrate that hypertonically induced microcages are similar in size and construction to the smallest of the "empty" cages found in the two in vitro preparations. Bar, 0.1 μm.

three types of clathrin assembly are compared in Fig. 6, where in vivo microcages can be seen to be relatively uniform in size and equivalent to the smallest of the clathrin cages found in the two in vitro preparations.

Previous investigators have found that the smaller cages in brain coated vesicle preparations are devoid of internal membranes, as judged by negative staining (8), deep-etch electron microscopy (17), and whole-mount cryo-electron microscopy (45, 46). Likewise, the microcages seen in hypertonically treated cells also appear to lack internal membranes. That is, when hypertonically treated cells were subjected to freeze-fracture analysis, we saw no evidence of small plasma

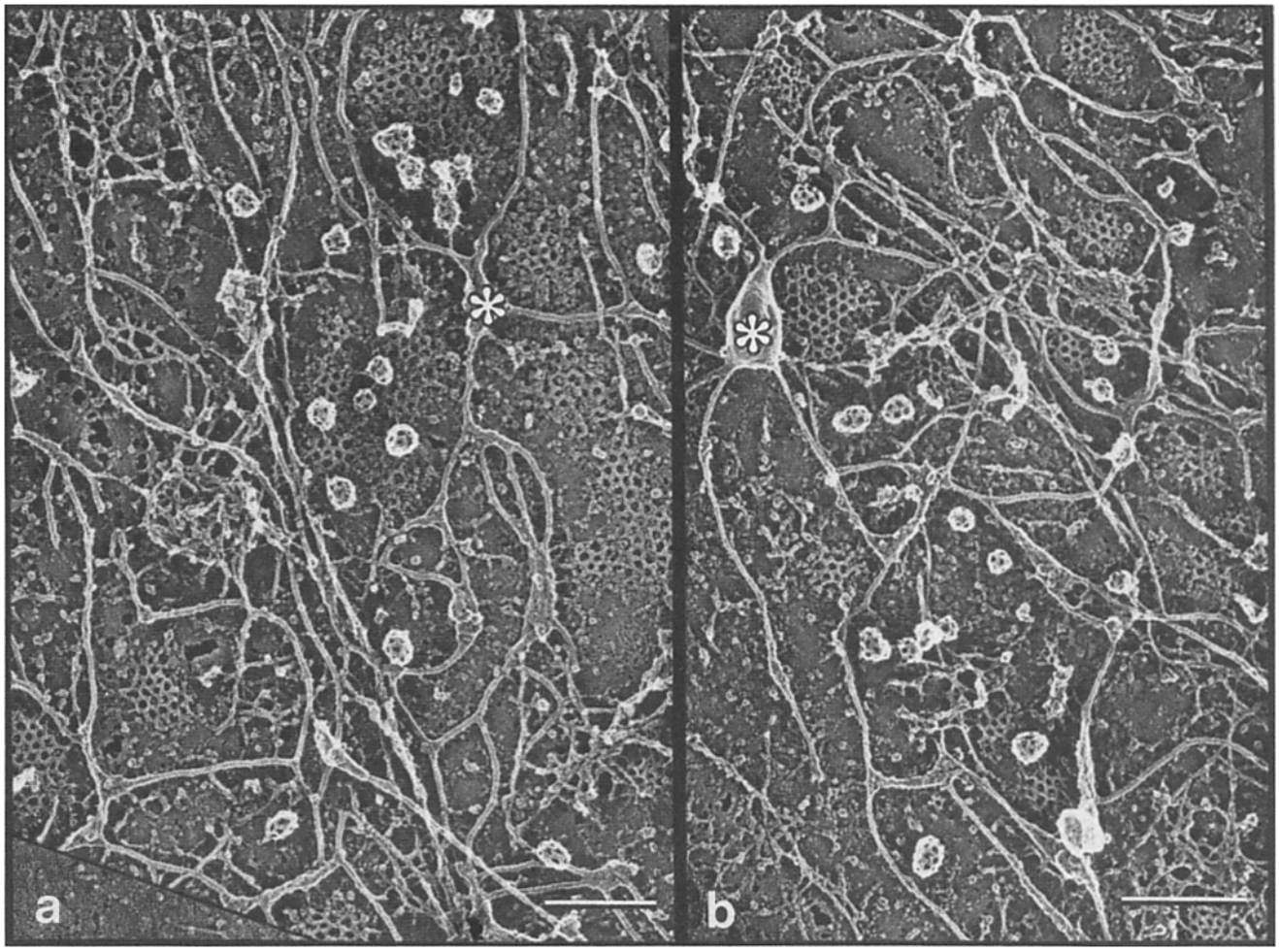

Figure 7. Human fibroblasts depleted of potassium for 1 h at 37°C by the hypotonic shock, K-free incubation procedure (24, 26). The result is essentially identical to that of hypertonic treatment (Fig. 4 *b*): numerous clathrin microcages are found amongst residual flat clathrin lattices. (Why the flat lattices are not entirely gone, as reported in reference 26, is not clear.) At the asterisks are some examples of the broad reticulum of branched, anastomotic membrane tubules that characteristically adheres to the plasma membrane of human fibroblasts (as opposed to chick fibroblasts). These tubules are not altered by hypertonicity. Bars, 0.2 μm.

membrane "pockets" of microcage size in the vicinity of coated pits (data not shown), though such pockets would be expected if microcages were able to enclose small portions of invaginated membrane.

Microcages Also Appear in K^+-depleted Cells

Previous studies by Larkin et al. (26) showed that small, round, vaguely polygonal structures also appear on the membrane of human fibroblasts after potassium depletion. However, this study used replicas of critical point dried membranes, which did not provide sufficient resolution to unanbiguously identify these new structures. We repeated these experiments and found that freeze dried membranes of K^+-depleted human fibroblasts looked essentially identical to the membranes of hypertonically treated cells (Fig. 7). In addition to displaying a residuum of reduced and flattened clathrin lattices, they also displayed large numbers of unusually small clathrin cages scattered across the inner membrane surface. Since freeze-fracture analysis again did not reveal any unusually small plasma membrane "pockets" in K^+-depleted cells (data not shown), these small cages undoubtedly correspond to the clathrin microcages seen here in hypertonicity.

Effects of Hypertonicity on the Distribution of LDL Receptors

Previous studies have shown that receptor-bound LDL on the surfaces of fibroblasts is readily visualized in freeze-etch replicas (15). Therefore, we have used the native ligand to study the distribution of LDL receptors under various conditions. When untreated human fibroblasts were chilled to 4°C and incubated with LDL, their surfaces displayed numerous clusters of LDL particles (Fig. 8). Usually these clusters were located in relatively flat indentations, although LDL clusters within deeper invaginations were also found (Fig. 8 *b*). Curiously, the LDL particles in these clusters often appeared to be aggregated or aligned into beads-on-a-string patterns. By contrast, in hypertonically treated cells the LDL

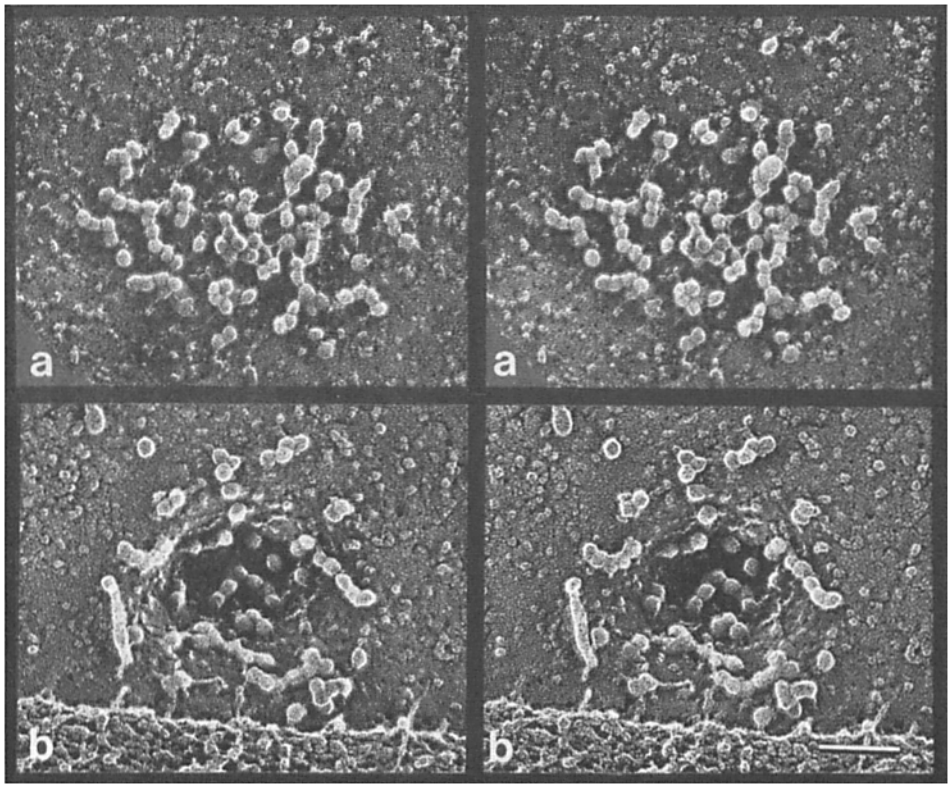

Figure 8. Stereo views of LDL clusters on control human fibroblasts, arranged to suggest the progress of invagination from *a* to *b*. Bar, 0.1 μm.

particles were dispersed on the cell surface; therefore, the receptors were not clustered in the absence of coated pits. Many of the LDL particles appeared to be present in groups of two particles (*circled* in Fig. 9 *a*). By quantitative analysis, the density of particles was ~55/μm² and 50–70% of the particles were dimeric.

A distinct reclustering of LDL receptors after the return to isosmotic buffer could also be followed in freeze dried cells. Thus, when hypertonically treated cells were incubated with LDL at 4°C and then shifted to 37°C in isosmotic buffer, clusters of particles reappeared within 2 min (Fig. 9 *b*). These clusters initially contained fewer LDL particles than clusters found in control cells (compare Fig. 9 *b* with Fig. 8). Moreover, at these early times of recovery, many LDL dimers remained dispersed on the cell surface. With longer times at 37°C, progressively more LDL particles appeared in the clusters (Fig. 9 *c*); by 10 min at 37°C, the clusters were often found to be deeply invaginated (Fig. 9 *d*). This time sequence of LDL particle clustering upon return to isotonic medium paralleled the recovery of coated pit lattices, as visualized on replicas of the inner cell surface (Table I).

Discussion

Potassium depletion and hypertonic treatment both inhibit receptor-mediated endocytosis (10, 24). Here, we show that both also cause a drastic reduction in normal coated pits and produce numerous "microcages" beneath the plasma membrane; e.g., both create the same changes in the distribution of clathrin. These changes are analyzed in more detail below.

The Formation of Microcages

Why two treatments as seemingly disparate as K^+ depletion and hypertonicity should lead to the same "salting out" of clathrin into microcages is not immediately obvious. However, in the accompanying paper (16), we show that experimental acidification of the cytoplasm causes an even more prompt formation of microcages. Moreover, we have found that hypertonicity creates some degree of cytoplasmic acidification (16) and others have found that potassium depletion also does so (29, 42). Still, it is not clear that the degree of acidification achieved by either treatment is sufficient to reach the threshold for microcage formation (pH 6.5; cf. reference 16 and Heuser, J. E., P. H. Schlesinger, and A. Roos, manuscript in preparation). Nor have we been able to consistently prevent microcage formation by blocking the acidification that normally accompanies cell shrinkage (personal observations). Thus, other factors besides lowered pH may also cause cytoplasmic clathrin to form microcages; obvious possibilities include the increases in protein and divalent-cation concentrations that accompany hypertonicity.

We know of only two previous reports on the in vivo accumulation of structures matching the description of microcages: one was in pancreatic acinar cells deprived of oxygen (33, 36) and the other in mosquito oocytes deprived of their normal supply of blood lipoprotein (39). Whether these conditions also involve some degree of cytoplasmic acidification remains to be seen, but seems quite likely. Furthermore, brain coated vesicle preparations such as those in Fig. 6 *c* contain a high proportion of microcages, and correspondingly, nerve cells are well-known to acidify postmortally. In any case, our current feeling is that microcage formation will

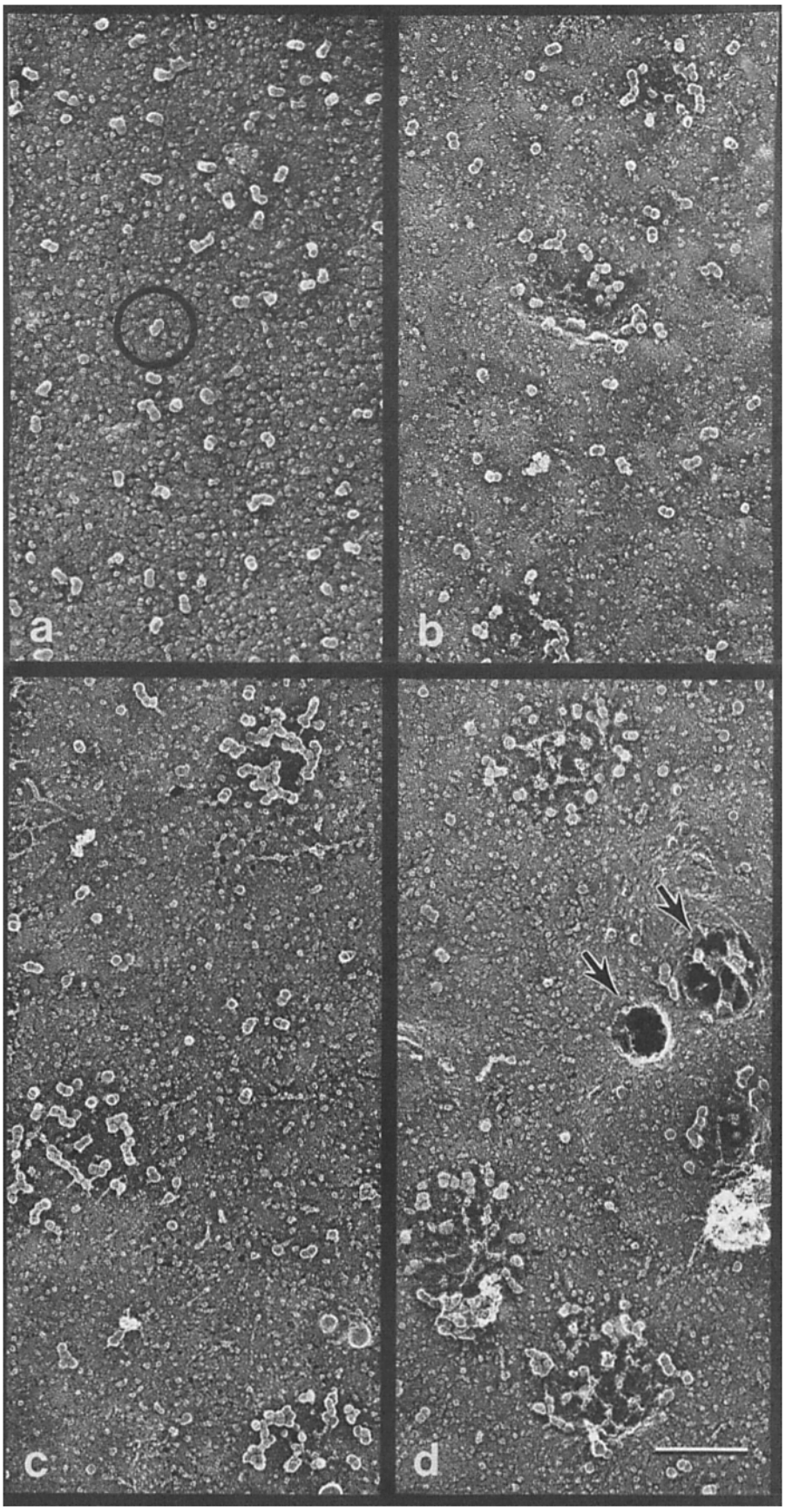

Figure 9. LDL receptor dispersion on human fibroblasts during and after treatment with 0.45 M hypertonic sucrose. (*a*) During treatment, normal LDL clusters are not found; instead LDL dimers (one of which is circled) are dispersed over the entire cell surface at a density of 30–80/ μm^2. (*b*) 2 min after return to isotonic medium, low density clusters of LDL begin to reappear. (*c*) 5 min after return to normal tonicity, LDL receptor clustering has progressed, presumably over newly formed coated pits. (*d*) 10 min after recovery, many of the receptor clusters have become deeply invaginated (*arrows*) presumably indicating they are pinching off to become coated vesicles. All panels at the same magnification, each representing ~ 2 μm^2 of cell surface area. Bar, 0.2 μm.

turn out to be a good indication of cytoplasmic acidification, and probably occurs via mechanisms similar to in vitro polymerization of clathrin by dialysis into acidic solutions (23, 38, 44, 47). This is discussed in more detail in the accompanying paper (16).

The Loss of Coated Pit Lattices

Even prolonged treatment with hypertonic media did not cause all of the coated pits to disappear from the cell surface (Table I). This differs from previous reports on the effects of potassium depletion (24, 26, 34); though in the current experiments, potassium depletion did not cause coated pits to disappear entirely either (Fig. 7). Nevertheless, we found that after either treatment the remaining coated pits were structurally abnormal in several respects. First, they were much smaller than normal, often consisting of only 5–10 hexagons. Second, they were much flatter than normal and often displayed no sign of curvature at all. Since these lattices remained present throughout hypertonic treatment (up to 60 min), they clearly were not able to support further endocytosis; but whether they were "residua" of arrested endocytosis or were involved in some entirely different function remains to be seen. For instance, since our analysis focused on portions of the plasma membrane that remained attached to the glass substratum, it was biased toward observing clathrin-undercoated attachment plaques (cf. references 1–3, 32, 35). If these in fact exist, they might be spots where clathrin could have an unusually high affinity for the plasma membrane, hence they might not depolymerize even in the face of severe loss of the clathrin involved in endocytosis. In any case, the present study agrees with previous reports in showing that big curved clathrin lattices, of the sort that look like they are involved in pinching off from the plasma membrane, essentially disappear during hypertonic treatment as well as during potassium depletion.

How Microcage Formation Could Lead to Loss of Coated Pits

Failure of clathrin lattices to form properly in hypertonic or potassium-depleted cells could represent either a loss of the normal supply of necessary substrates for lattice formation or a disruption of the normal signals for polymerization. We favor the former possibility for two reasons. First, on simple intuitive grounds, the abrupt appearance of microcages in hypertonic cells would suggest that signals for clathrin polymerization are in fact enhanced, not diminished. Normal cells maintain a pool of cytoplasmic clathrin that behaves as if it is soluble (14, 28); there is no indication that the pool is normally in the form of small microcages. Indeed, there is immunological evidence that this pool is not polymerized (7, 14, 28, 34). Thus, the appearance of microcages in hypertonic cells appears to represent a shift toward polymerization, which might also have been manifest as an enhancement of coated pit formation, not a reduction.

Second, on more quantitative grounds, the magnitude of microcage formation appears to be sufficiently great to consume the normal cytoplasmic pool; this would of course interrupt further clathrin lattice formation and thereby halt receptor-mediated endocytosis. The quantitative basis for concluding that microcage formation consumes the cytoplasmic pool of clathrin is as follows: (*a*) The normal size of the pool of unpolymerized clathrin in typical cultured cells (e.g., the portion that is Triton X-100–extractable) is ~50% of the total (~2×10^5 molecules) (14, 28). (*b*) The normal size of the polymerized pool, based on the numbers of coated pits seen in normal cells (but neglecting the contribution of Golgi-associated coated vesicles) also approaches 2×10^5 molecules. This has been measured (14), but also can be derived as follows: coated pits represent 1–2% of the cell surface (4–6), so a typical fibroblast with a surface area of 2,500 μm^2 will have ~1,000–2,000 coated pits present at any one time. Its coated pits measure 0.18–0.24 μm in diameter (and correspondingly, the final coated vesicles in fibroblasts measure 0.9–0.12 μm in diameter) a size range that would require 80–140 clathrin triskelia per coat (cf. references 15, 17). The total number of triskelia thus tied up in all the coated structures on any one fibroblast is $0.8–2.8 \times 10^5$ molecules ($80 \times 1{,}000$ to $140 \times 2{,}000$). (*c*) After hypertonic treatment, the total number of coated pits per cell diminishes by ~50% (Table I), while their average size diminishes to ~0.14 μm in diameter, equivalent to no more than ~50 triskelia per residual coat. This represents a drop to ~$0.5–0.75 \times 10^5$ triskelia in lattices on the surfaces of hypertonic cells, equivalent to a release of ~$1.0–1.5 \times 10^5$ triskelia per cell. (*d*) The abundance of microcages in hypertonic cells, based solely on counts of the ones that stick to the plasma membrane during sonication and freeze-etching, is ~5,000–7,500 per cell (~2–3 microcages/μm^2 of cell surface; cf. Fig. 4 *b*). Since each microcage measures 50–60 nm, each must contain between 28 and 36 triskelia (8, 17, 38). This means that microcages tie up $1.4–2.7 \times 10^5$ triskelia per cell (e.g., $20 \times 5{,}000$ to $36 \times 7{,}500$), more than enough to account for all the triskelia that are freed by lack of involvement in coated pits (*c* above). (Another way to appreciate this is to remember that each normal coated pit involves ~120 triskelia while each microcage ~30 triskelia, so if one simply derived from the other, ~4 microcages should appear for every coated pit that disappears. In fact, coated pits do not completely disappear in hypertonic cells, yet microcages become more than four times as abundant as the original population of coated pits (2–3 microcages/μm^2 in hypertonic cells vs. 1 coated pit/2 μm^2 in normal cells). (*e*) The total number of microcages in hypertonic cells is probably much greater than the number found on the plasma membrane after sonication; immunofluorescence data such as Fig. 3 strongly suggests this. Hence, microcages would seem to make major inroads into the soluble pool of clathrin, as well as consuming the triskelia normally involved in coated pits.

There are a number of uncertainties in the above lines of reasoning, largely resulting from the degree of variability in these parameters seen from cell to cell. Not until individual cells can be analyzed both before and after hypertonic treatment will the actual extent of clathrin lattice conversion be obvious. Nevertheless, our current impression is that microcages become sufficiently abundant to account for all loss of clathrin from normal lattices as well as to deplete the normal cytoplasmic pool. Hypertonicity (and by analogy, potassium depletion) would thus appear to arrest normal coated pit formation by creating an abnormally great amount of clathrin polymerization in the wrong place. The normal control of clathrin polymerization at receptor-rich sites on the plasma membrane is apparently overridden, and thus receptor-mediated endocytosis stops.

Dynamics of Receptor Clustering

Previously, Larkin et al. (24, 26) showed by thin sectioning that potassium depletion led to complete dispersion of LDL–ferritin on the surface of human fibroblasts. Hypertonic treatment produced the same receptor dispersion, as indicated by the distribution of LDL particles on the surface of the cells studied here. In the dispersed state, the LDL particles were predominantly arranged into groups of two particles. Since LDL particles adsorbed to mica were monomeric (data not shown), most likely the dimeric LDL reflects the presence of receptors that are self associated into groups of two on the cell surface. Van Driel et al. (43) used bivalent cross-linkers to show that a significant proportion of the LDL receptors on the surface of Chinese hamster ovary (CHO) cells transfected with a cDNA for the normal human receptor exist as dimers. Similarly, the receptor for *N*-acelylglucosamine–terminated glycoproteins in chickens appears to exist as multimers on the cell surface (27). Whereas it is difficult to quantify the number of receptors that are self associated using cross-linking techniques (43), our results indicates that in human fibroblasts >50% are dimeric.

The first sign of receptor reclustering upon return to isotonic media turns out to be the appearance of broad depressions containing relatively few LDL particles (Fig. 9 *b*). LDL particles reach their maximum concentration in these depressions only several minutes later (Fig. 9 *c*). This temporal sequence suggests that as soon as nascent coated pits form, they gain an ability to sequester LDL receptors, but receptors move relatively slowly into the "sticky" loci they create in the plasma membrane. More definitive conformation that this is the natural sequence of coated vesicle formation will await the development of a technique that will permit simultaneous visualization of receptor clusters and clathrin lattices on opposite sides of the membrane. With such a technique, the methods of blocking endocytosis described here should prove useful in dissecting apart the natural sequence of clathrin lattice formation and receptor clustering.

We wish to thank Robyn Roth and Melisse Reichman for skillfully preparing all the freeze-etch replicas used in this study, Cary Colman for photography, and Jan Jones for typing. Thanks also to Drs. T. Kirchhausen (Harvard Medical School) and J. Keen (Temple University Medical School) for supplying the coated vesicles and clathrin cages displayed in Fig. 6, as well as for their many helpful discussions.

Supported by United States Public Health Service grants to J. Heuser (GM-29647) and R. Anderson (HL-20948).

Received for publication September 13, 1988, and in revised form 17 October 1988.

References

1. Deleted in proof.
2. Aggeler, J., and Z. Werb. 1982. Initial events during phagocytosis by macrophages viewed from outside and inside the cell: membrane-particle interactions and clathrin. *J. Cell Biol.* 94:613–623.
3. Aggeler, J., J. E. Heuser, and Z. Werb. 1982. Presence of clathrin at adhesion sites in phagocytosing macrophages. *Annu. Proc. E. M. Soc. Amer.*, 40th. 114–117.
4. Anderson, R. G. W., and J. Kaplan. 1983. Receptor-mediated endocytosis. *Mod. Cell Biol.* 1:1–52.
5. Anderson, R. G. W., E. Vasile, R. J. Mello, M. S. Brown, and J. L. Goldstein. 1978. Immunocytochemical visualization of coated pits and vesicles in human fibroblasts: relation to low density lipoprotein receptor distribution. *Cell.* 15:919–933.
6. Anderson, R. G. W., J. L. Goldstein, and M. S. Brown. 1980. Fluorescence visualization of receptor-bound low density lipoprotein in human fibroblasts. *J. Recept. Res.* 1:17–39.
7. Brodsky, F. M. 1985. Clathrin structure characterized with monoclonal antibodies I & II. *J. Cell Biol.* 101:2047–2062.
8. Crowther, R. A., J. T. Finch, and B. M. F. Pearse. 1976. On the structure of coated vesicles. *J. Cell Biol.* 103:785–798.
9. Daiss, J. L., and T. F. Roth. 1983. Isolation of coated vesicles: comparative studies. *Methods Enzymol.* 98:337–349.
10. Daukas, G., and S. H. Zigmond. 1985. Inhibition of receptor-mediated but not fluid-phase endocytosis in polymorphonuclear leucocytes. *J. Cell Biol.* 101:1673–1679.
11. Davoust, J., J. Gruenberg, and K. E. Howell. 1988. Two threshold values of low pH block endocytosis at different stages. *EMBO (Eur. Mol. Biol. Organ.) J.* 6(12):3601–3609.
12. Goldstein, J., S. K. Basu, and M. S. Brown. 1983. Receptor-mediated endocytosis of low-density lipoprotein in cultured cells. *Methods Enzymol.* 98:241–260.
13. Goodenough, U., and J. Heuser. 1984. Structural comparison of purified dynein proteins with in situ dynein arms. *J. Mol. Biol.* 180:1083–1118.
14. Goud, B., C. Huet, and D. Louvard. 1985. Assembled and unassembled pools of clathrin: a quantitative study using enzyme assay. *J. Cell Biol.* 100:521–527.
15. Heuser, J. E. 1980. Three-dimensional visualization of coated vesicle formation in fibroblasts. *J. Cell Biol.* 84:560–583.
16. Heuser, J. E. 1989. Effects of cytoplasmic acidification on clathrin lattice morphology. *J. Cell Biol.* 108:401–411.
17. Heuser, J. E., and T. Kirchhausen. 1985. Deep etch views of clathrin assemblies. *J. Ultrastruct. Res.* 92:1–27.
18. Heuser, J. E., and M. W. Kirschner. 1980. Filament organization revealed in platinum replicas of freeze-dried cytoskeletons. *J. Cell Biol.* 86: 212–234.
19. Heuser, J. E., and T. S. Reese. 1973. Evidence for recycling of synaptic vesicle membrane during transmitter release at the frog neuromuscular junction. *J. Cell Biol.* 57:315–344.
20. Heuser, J. E., T. S. Reese, C. Y. Jan, Y. N. Jan, M. J. Dennis, and L. Evans. 1979. Synaptic vesicle exocytosis captured by quick freezing and correlated with quantal transmitter release. *J. Cell Biol.* 81:275–300.
21. Deleted in proof.
22. Ilondo, M. M., P. J. Courtoy, D. Geiger, J-L. Carpentier, G. G. Rousseau, and P. De Meyts. 1986. Intracellular potassium depletion in IM-9 lymphocytes suppresses the slowly dissociating component of human growth hormone binding and the down-regulation of its receptors but does not affect insulin receptors. Proc. Natl. Acad. Sci. USA. 83:6460–6464.
23. Keen, J. H., M. C. Willingham, and I. H. Pastan. 1979. Clathrin-coated vesicles: isolation, dissociation and factor-dependent reassociation of clathrin baskets. *Cell.* 16:303–312.
24. Larkin, J. M., M. S. Brown, J. L. Goldstein, and R. G. W. Anderson. 1983. Depletion of intracellular potassium arrests coated pit function and receptor-mediated endocytosis in fibroblasts. *Cell.* 33:273–285.
25. Larkin, J. M., W. C. Donzell, and R. G. W. Anderson. 1985. Modulation of intracellular potassium and ATP: effects on coated pit function in fibroblasts and hepatocytes. *J. Cell Physiol.* 124:372–378.
26. Larkin, J. M., W. D. Donzell, and R. G. W. Anderson. 1986. Potassium dependent assembly of coated pits: new coated pits form as planar clathrin lattices. *J. Cell Biol.* 103:2619–2627.
27. Loeb, J. A., and K. Drickamer. 1987. The chicken receptor for endocytosis of glycoproteins contains a cluster of N-acetylglucosamine-binding sites. *J. Biol. Chem.* 262:3022–3029.
28. Louvard, D., C. Morris, G. Warren, K. Stanley, F. Winkler, and H. Reggio. 1983. A monoclonal antibody to the heavy chain of clathrin. *EMBO (Eur. Mol. Biol. Organ.) J.* 2:1655–1664.
29. Madshus, I. H., T. I. Tonnessen, S. Olsnes, and K. Sandvig. 1987. Effect of potassium depletion of Hep 2 cells on intracellular pH and on chloride uptake by anion transport. *J. Cell Physiol.* 131:6–13.
30. Madshus, I. H., K. Sandvig, S. Olsnes, and B. van Deurs. 1987. Effect of reduced endocytosis induced by hypotonic shock and potassium depletion on the infection of Hep 2 cells by Picornaviruses. *J. Cell Physiol.* 131:14–22.
31. Marsh, M., and A. Helenius. 1980. Adsorptive endocytosis of semliki forest virus. *J. Mol. Biol.* 142:439–454.
32. Maupin, P., and T. D. Pollard. 1983. Improved preservation and staining of HeLa cell actin filaments, clathrin coated membranes, and other cytoplasmic structures by tannic acid-glutaraldehyde-saponin fixation. *J. Cell Biol.* 96:51–62.
33. Merisco, E. M., M. Fletcher, and G. E. Palade. 1986. The reorganization of the Golgi complex in anoxic pancreatic acinar cells. *Pancreas.* 1:95–109.
34. Moya, M., A. Dautry-Varsat, B. Goud, D. Louvard, and P. Boquet. 1985. Inhibition of coated pit formation in Hep_2 cells blocks the cytotoxicity of diphtheria toxin but not that of ricin toxin. *J. Cell Biol.* 101:548–559.
35. Nicol, A., and M. V. Nermut. 1987. A new type of substratum adhesion structure in NRK cells revealed by correlated interference reflection and electron microscopy. *Eur. J. Cell Biol.* 43:348–357.
36. Deleted in proof.
37. Pearse, B. M. F. 1975. Coated vesicles from pig brain: purification and biochemical characterization. *J. Mol. Biol.* 97:93–98.

38. Pearse B. M. F., and R. A. Crowther. 1987. Structure and assembly of coated vesicles. *Annu. Rev. Biophys. Biophys. Chem.* 16:49–68.
39. Raikhel, A. S. 1984. Accumulations of membrane-free clathrin-like lattices in the mosquito oocyte. *Eur. J. Cell Biol.* 35:279–283.
40. Sandvig, K., A. Sundan, and S. Olsnes. 1985. Effect of potassium depletion of cells on their sensitivity to diphtheria toxin and pseudomonas toxin. *J. Cell Physiol.* 124:54–60.
41. Sandvig, K., S. Olsnes, O. W. Peterson, and B. van Deurs. 1987. Acidification of the cytosol inhibits endocytosis from coated pits. *J. Cell Biol.* 105:679–689.
42. Samuelson, A. C., R. J. Stockert, A. B. Novikoff, P. M. Novikoff, J. C. Saez, D. C. Spray, and A. W. Wolkoff. 1988. Influence of cytosolic pH on receptor-mediated endocytosis of asialoorosomucoid. *Am. J. Physiol.* 254:C829–C838.
43. van Driel, I. R., C. G. Davis, J. L. Goldstein, and M. S. Brown. 1987. Self-association of the low density lipoprotein receptor mediated by the cytoplasmic domain. *J. Biol. Chem.* 262:16127–16134.
44. van Jaarsveld, P. P., P. K. Nandi, R. E. Lippoldt, H. Saroff, and H. Edelhoch. 1981. Polymerization of clathrin protomers into basket structures. *Biochemistry.* 20:4129–4135.
45. Vigers, G. P. A., R. A. Crowther, and B. M. F. Pearse. 1986. Three-dimensional structure of clathrin cages in ice. *EMBO (Eur. Mol. Biol. Organ.) J.* 5:529–534.
46. Vigers, G. P. A., R. A. Crowther, and B. M. F. Pearse. 1986. Location of the 100 Kd-50 accessory proteins in clathrin coats. *EMBO (Eur. Mol. Biol. Organ.) J.* 5:2079–2085.
47. Woodward, M. P., and T. F. Roth. 1979. Influence of buffer ions and divalent cations on coated vesicle disassembly and reassembly. *J. Supramol. Struct.* 11:237–250.
48. Zaremba, S., and J. H. Keen. 1983. Assembly polypeptides from coated vesicles mediate assembly of unique clathrin coats. *J. Cell Biol.* 97: 1339–1347.